CHARACTERIZATION OF OBSERVED TRENDS IN THE ERROR OF THE SUNY SATELLITE IRRADIANCE MODEL

Anders Nottrott
UC San Diego, MAE
9500 Gilman Dr, EBU II
La Jolla, CA 92093-0411, USA

Jan Kleissl
(Corresponding author)
UC San Diego, MAE
9500 Gilman Dr, EBU II
La Jolla, CA 92093-0411, USA
jkleissl@ucsd.edu

ABSTRACT

Remote sensing models are a powerful approach to estimating surface irradiance at high spatial resolution over large geographic areas. In this paper we evaluate the accuracy of a national hourly irradiance dataset for the United States which was derived from Geostationary Operational Environmental Satellite (GOES) data. The modeled dataset is held in the National Solar Radiation Database (NSRDB) and was produced using the Perez *et al* 2002 satellite-to-irradiance model (SUNY). We test the accuracy of the model by comparing the modeled dataset to irradiance data measured on the ground obtained from the California Irrigation Management and Information System (CIMIS). Generally we find that the satellite model is in agreement with ground data, but significant errors in the modeled data are observed on summer mornings and year-round during the evening. From our analysis it is apparent that these errors are independent and are generated by different physical processes in the atmosphere. The summer morning errors are related to problems with model parameterization of dense cloud cover and year-round evening errors are attributed to enhanced scattering of solar radiation at low sun altitude angles.

1. INTRODUCTION

As the number of installations of photovoltaic (PV) and other solar energy conversion systems grows worldwide, the accuracy, spatial and temporal resolution and availability of irradiance data become increasingly important. Accurate, site specific solar resource assessments are required to extrapolate future power potential and perform economic cost/benefit analyses for PV systems. The site specific solar resource is frequently evaluated by conducting a statistical analysis of an historical timeseries of irradiance data to develop estimates about average insolation conditions at a particular site during a typical meteorological year (TMY). Irradiance data measured at sites on the ground can provide accurate, reliable datasets with high temporal resolution (i.e. the frequency of measurements is on the order of 1 s to 1 hr), however, it is prohibitively expensive to deploy in situ irradiance sensor networks at high spatial density over large geographic regions. As a result the spatial resolution of irradiance data obtained from such networks will be insufficient to capture geographic variability in irradiance at the regional, national and global scale. Satellite remote sensing models of irradiance provide an excellent solution to the problem of limited spatial resolution of in situ sensor networks while still maintaining acceptable temporal resolution (i.e. the frequency of measurements is on the order of 1 to 3 hrs). Many attempts have been made to model surface irradiance from geostationary weather satellites (Cano *et al.* 1986, Schmetz 1989, Zelenka *et al.* 1999, Perez *et al.* 2002 and Martins *et al.* 2007). In the United States the National Renewable Energy Laboratory (NREL) maintains the National Solar Radiation Database (NSRDB) which includes a modeled hourly irradiance dataset for the entire United States developed using the Perez *et al.* 2002 model (this model is hereafter referred to as SUNY). The NSRDB SUNY dataset consists of modeled irradiance data for the period from 1998-2005 at 0.1° resolution (0.1° is approximately 10km in the United States). In this paper we validate global horizontal irradiance (GHI) values the NSRDB SUNY dataset against GHI data from 26 ground stations in the state of California in order to evaluate the accuracy of the satellite derived irradiances.

2. DATA

The analysis presented in this paper is a continuation of our previous validation study of the NSRDB SUNY dataset (Nottrott and Kleissl 2010). The NSRDB SUNY dataset was derived using visible images from Geostationary Operational Environmental Satellites (GOES). The SUNY model converts satellite return radiance counts to surface irradiance values by estimating cloud cover in terms of a cloud index (CI) for each pixel in the GOES image. This CI is then used in a transmittance function to modulate a modeled value of the clear sky irradiance for each pixel in the image. The SUNY model also incorporates information about atmospheric turbidity, ground snow cover, ground specular reflectance characteristics, and individual pixel sun-satellite angle effects to improve hourly estimates for surface irradiance.

GHI values from NSRDB SUNY dataset were compared with GHI data from 26 ground stations across the state of California, USA. The ground stations are part of a coordinated sensor network called the California Irrigation Management and Information System (CIMIS) (CIMIS 2010). GHI is measured at each of these sites using a Li-Cor LI200SZ photodiode pyranometer and recorded as the hourly average of 60 GHI measurements made within the hour. Extensive data quality control (QC) was performed on the CIMIS measurements to ensure that only the highest quality ground data was included in this analysis. All ground stations included in the analysis had at least one full year of continuously valid GHI data and the average length of a single CIMIS GHI data timeseries was 5 years among all 26 sites.

We related observed trends in the error of the satellite derived irradiance to climatologies of cloud cover at each ground station. Cloud cover data was obtained from the National Climactic Data Center (NCDC) Integrated Surface Dataset (DSI-3505) (NCDC 2008).

3. ANALYSIS

3.1 Definition of Variables

We analyze the error in the satellite modeled data in terms of the mean bias error (MBE) between the NSRDB SUNY and the CIMIS ground data.

$$MBE = (1/N)\sum_{n=1}^{N}(GHI_{SUNY,n} - GHI_{CIMIS,n}) \qquad \text{(Eq. 1)}$$

In Eq. 1 *GHI* represents an hourly GHI value from the subscripted dataset, *N* is the number of data points in the timeseries and the MBE is given in units of W m^{-2}. The percent MBE was computed by normalizing the summand of Eq. 1 by $GHI_{CIMIS,ave}$, where $GHI_{CIMIS,ave}$ represents the mean value of GHI measured at the ground station averaged for the appropriate time interval (e.g. an annual MBE is normalized by the year-round $GHI_{CIMIS,ave}$ and a monthly-hourly MBE (e.g. see Fig. 1) is normalized by $GHI_{CIMIS,ave}$ for the corresponding hour averaged over the month). In this analysis cloud cover is quantified in two ways. The first definition of cloud cover is sky cover fraction (SCF) which is measured in the DSI-3505 using four descriptors that correspond to the amount of sky that is covered by opaque clouds. Clear (CLR, SCF=0) indicates no cloud cover, while scattered (SCT, 1/8 to 4/8, SCF=0.31), broken (BKN, 5/8 to 7/8, SCF=0.75) and overcast (OVC, 8/8, SCF=1.0) indicate fractional sky coverage. The average SCF was assigned to each indicator to obtain a numerical dataset. We also examine the dependence of error in the satellite derived irradiance on the clearness index (kt*) which is defined after Lorenz *et al*. 2009 as the hourly ratio of the satellite derived irradiance to modeled clear sky irradiance.

$$kt^{*} = GHI_{SUNY,n}/GHI_{SKC,n} \qquad \text{(Eq. 2)}$$

In Eq. 2 $GHI_{SUNY,n}$ is an hourly GHI value in the NSDRB SUNY dataset and $GHI_{SKC,n}$ is the modeled clear sky irradiance during the same hourly period. The clear sky irradiance is computed from a geometric model based on the approach taken by Snyder and Eching 2002.

3.2 Observed Trends in Error of Satellite Derived Data

a)

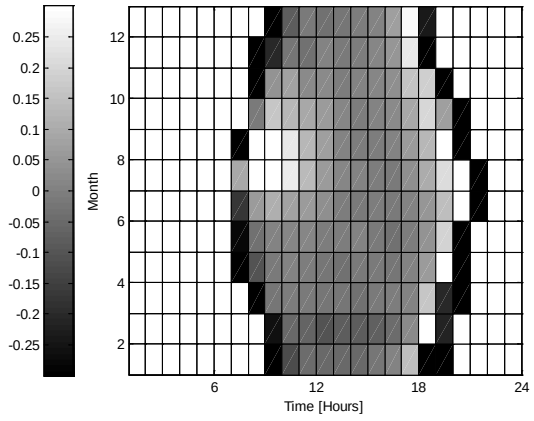

b)

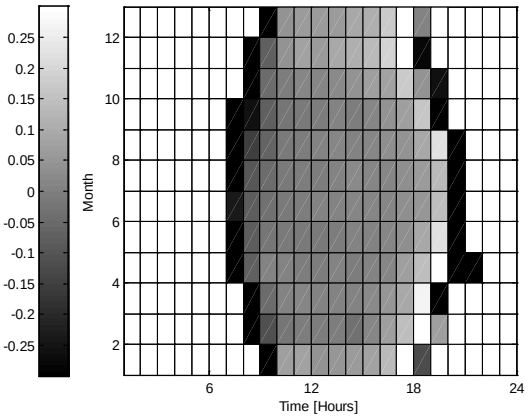

c)

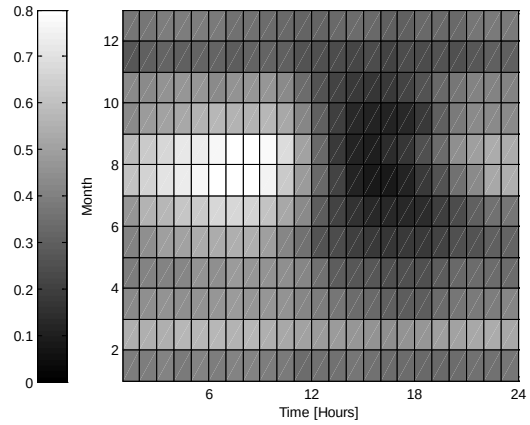

d)

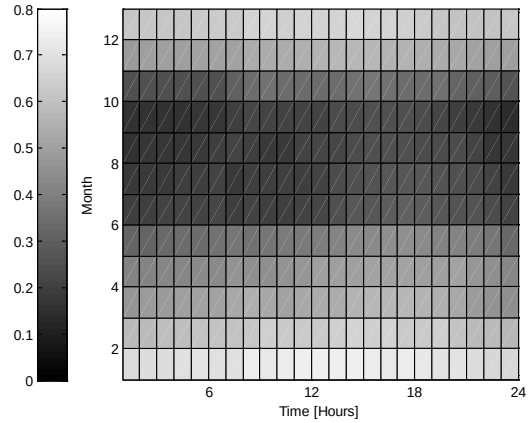

Fig. 1: MBE [%/100] between SUNY model and CIMIS data averaged hourly by month for **(a)** a typical coastal station CIMIS #129, 5.7 km from the coast and **(b)** a typical inland station CIMIS #002, 122 km from the coast. SCF [-] averaged hourly by month at **(c)** Watsonville airport near CIMIS #129 and **(d)** Lemoore NAS near CIMIS #002

Fig. 1a,b illustrate temporal trends of MBE in the SUNY modeled data for a typical site near the coast (CIMIS #129) and a typical site far from the coast (CIMIS #002). Large negative MBE that occurs in the early morning and late evening may be ignored for practical purposes because the magnitude of the GHI during these hours is small (< 100 W m^{-2}). Good agreement between the modeled and measured data is observed year-round except for two periods when satellite derived irradiances are significantly larger than the values measured on the ground. In Fig. 1a large positive MBE is observed during the summer in the morning. In both Fig. 1a,b large positive MBE occurs year-round in the evening. Fig. 1c,d show average patterns of cloudiness for CIMIS sites #129 and #002 respectively. Fig. 1c indicates that summer morning errors at the costal site occur at the same time when dense cloud cover is present, which suggests that these errors are caused by marine layer clouds that develop regularly at this time of year near the coast in California. Fig. 1c,d provide no indication that the evening errors observed at both inland and coastal sites are related to patterns of cloudiness.

3.3 MBE as a function of cos(SZA) and kt*

We further investigate the cause of these errors by examining the MBE as a function of the solar zenith angle (SZA) and the clearness index for different times of the year in Fig. 2. Fig. 2a shows this result for the summer morning errors observed in Fig. 1a, and it appears that in this case MBE depends on both cos(SZA) and kt*. Year-round evening data is plotted Fig. 2b to visualize the cos(SZA)-kt* dependence of the evening errors observed in Fig. 1a,b which did not appear to be related to cloudiness. Fig. 2b suggests that the evening errors are only a function of cos(SZA) and are not strongly dependant on kt*.

a)

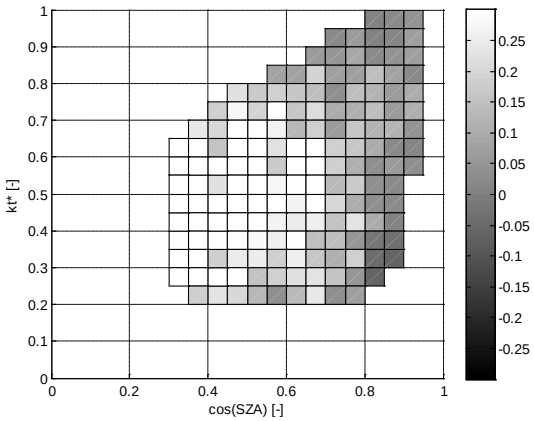

b)

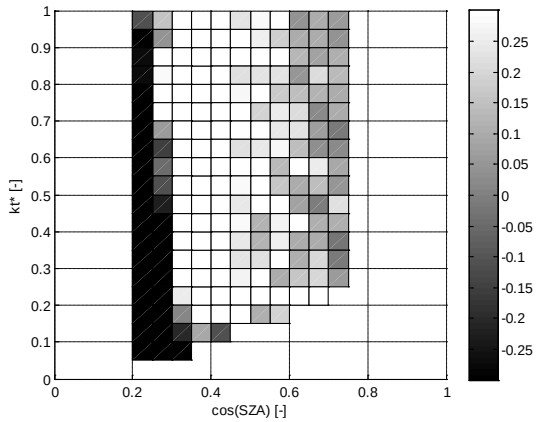

Fig. 2: Hourly SUNY MBE [%/100] as a function of cos(SZA) and kt* for **(a)** summer morning June-Sept, 701-1300PST and **(b)** year-round evening with 38°<SZA<102.3° at 26 stations in California. The data in this figure is averaged over 26 ground stations.

a)

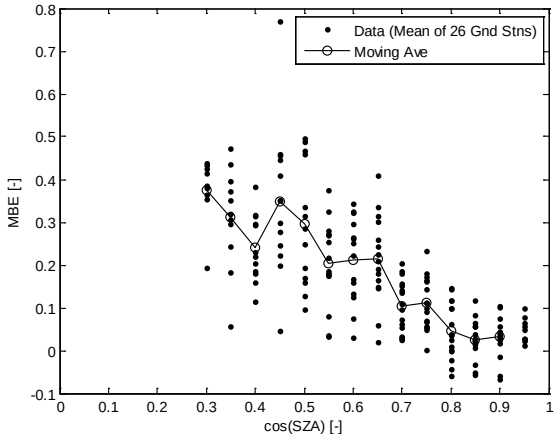

b)

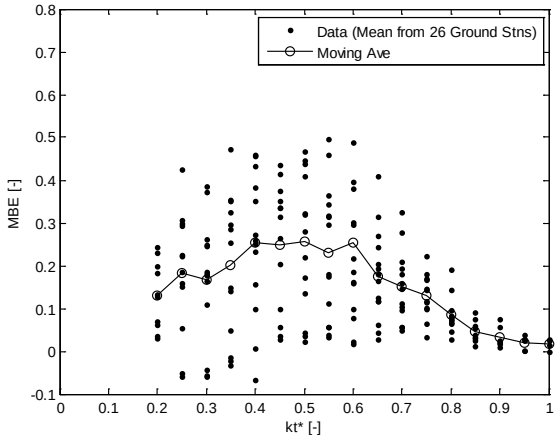

c)

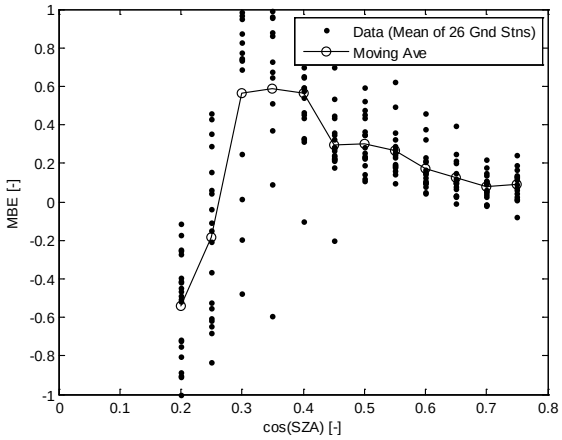

d)

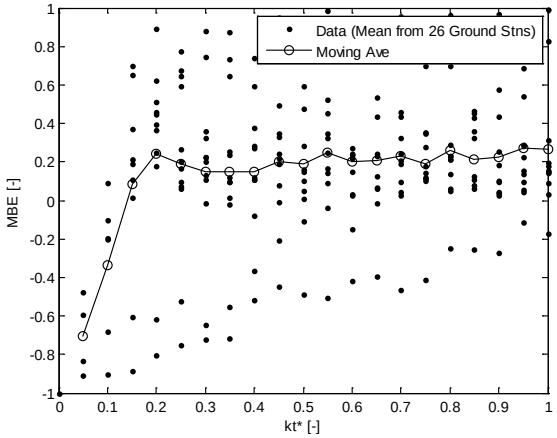

Fig. 3: Hourly SUNY MBE [%/100] as a function of **(a)** cos(SZA) and **(b)** kt* for summer morning June-Sept, 701-1300PST; **(c)** cos(SZA) and **(d)** kt* for year-round evenings with 38°<SZA<102.3° at 26 CIMIS stations in California. The line is a moving average of the data points.

The trends observed in Fig. 2 are better quantified by graphing MBE one-dimensionally as a function of only cos(SZA) or kt* for summer morning and year-round evening data separately (Fig. 3). Fig. 3a,b confirm that summer morning MBE increases with SZA and decreases with increasing kt*. Fig. 3c,d show that year-round evening MBE depends on cos(SZA) but is independent of kt*. We also note that in Fig. 3c MBE increases with SZA for cos(SZA)>0.2, at cos(SZA)=0.3 the slope of the moving average line changes sign and MBE becomes decreases with increasing SZA for cos(SZA)<0.3.

3.4 MBE as a function of cos(SZA)*sign(azimuth-180°) and kt*

The analysis of Fig. 1 and Fig. 3 suggests that observed summer morning and year-round evening MBE in the

NSRDB SUNY dataset are fundamentally different in nature and were generated by two independent physical processes. In order to parameterize the morning and evening errors independently over the entire year we define a new variable *cos(SZA)*sign(azimuth-180°)* which is used to distinguish morning and evening GHI values (Fig. 4). The positive MBE pattern observed in Fig. 2a for summer morning clouds is still evident when all data are used, and the error extends to sunrise. Likewise the evening errors appear as a region of negative MBE for cos(SZA) < 0.25 and positive MBE for 0.25 < cos(SZA) < 0.5, independent of kt*. Around noon, both in the morning and afternoon the MBEs are smaller and a more noisy pattern emerges with a trend to slightly larger MBE for small kt*.

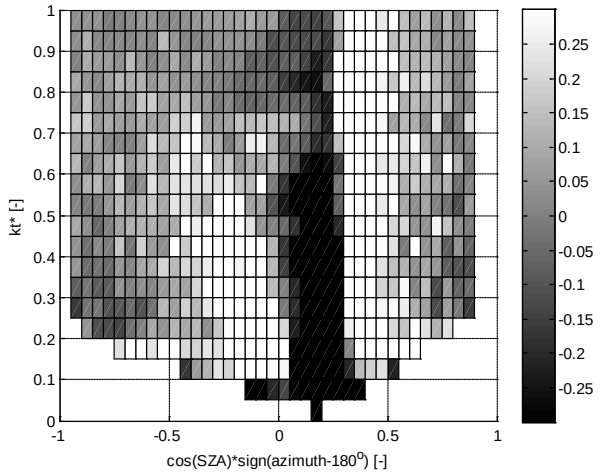

Fig. 4: Hourly SUNYMBE [%/100] as a function of cos(SZA)*sign(azimuth-180°) for the entire year at 26 CIMIS stations in California. Morning data (i.e. data before solar noon) appear on the left side of the plot where cos(SZA)*sign(azimuth-180°)<0. Afternoon data (i.e. data after solar noon) appears on the right side of the plot where cos(SZA)*sign(azimuth-180°)>0. If the x axis were time it would go from 1159 PST to sunrise (cos SZA = 0-) and then from sunset (cos SZA = 0+) to 1201 PST.

4. CONCLUSIONS AND FUTURE WORK

Generally we find that the SUNY model produces accurate estimates of irradiance, but our analysis helps to identify some persistent flaws in the modeled data that depend on season and time of day. Large positive MBEs in the NSRDB SUNY dataset are observed at coastal ground stations during summer mornings and large positive MBEs are present year-round in the evenings at all ground stations. Based on the climatologies of cloudiness presented in Fig. 1c,d for coastal and inland sites we believe that summer morning errors are caused by low altitude marine layer clouds that occur regularly during this time year throughout coastal California. This hypothesis is supported by Fig. 3b which suggests that summer morning errors increase as cloudiness increases. Fig. 3a shows that summer morning error also increases with SZA. This is probably related to a non-linear decrease in the amount Mie scattering of incident solar radiation that occurs when sunlight is incident on a low cloud layer. Near sunrise as the solar altitude increases the atmospheric optical thickness through which incident solar radiation travels to reach earth's surface decreases non-linearly. Because opaque clouds are present in the atmosphere at this time, the distance through which incident solar radiation must travel in the cloud will also decrease non-linearly. The SUNY model does not seem to properly account for this effect.

Year round evening MBE, however, cannot be explained by patterns of cloudiness (Fig. 1c,d). We believe that these errors are related to the geography of the western United States. In the western U.S. the sun rises in the east over the land mass of the North American continent and sets in the west over the Pacific Ocean. In general terms physical intuition suggests that the column water vapor content in the lower atmosphere over the North American land mass will be lower than the column water vapor content in the lower atmosphere over the Pacific Ocean. This is because more water is available at the surface for evaporation over the ocean than over land. Remote sensing studies of water vapor in the lower atmosphere (surface-700 mb, Randel *et al* 1996 and Sudradjat *et al.* 2004) show that on average atmospheric water vapor content is lower over North America than it is over the Pacific Ocean in the northern hemisphere (for latitude < 45°). Following this reasoning, on the west coast of the U.S., the optical path through a clear atmosphere along which incident solar radiation travels will be relatively "dry" in the morning and "wet" in the evening (i.e. incident solar radiation passing through the atmosphere encounters less water vapor in the morning than in the evening). Thus the amount of Rayleigh and Mie scattering of incident solar radiation would be greater than expected in the evening resulting in an overestimation by the SUNY model of the amount of irradiance arriving at the surface of the earth. This hypothesis is supported by Fig. 3c,d which show that year-round evening MBE depends only on cos(SZA) and not kt* and provides an explanation for why we do not see this kind of error during the morning. Although the SUNY model accounts for aerosol and water vapor via the Linke turbidity factor (T_L) in the modified Kasten clear sky model, T_L data input for the NSRDB SUNY data set was based on global scale, monthly average broadband turbidity data derived from satellites at nadir. This method for incorporating atmospheric turbidity would not allow the model to correctly parameterize the difference in atmospheric composition which is created by the regional geography of western North America.

Future work in this analysis will focus on developing a correction for the NSRDB SUNY dataset using the result presented in Fig. 4. This characterization of the observed errors in the modeled data will allow us to "simultaneously" estimate and correct model errors that are produced by two independent phenomena.

5. ACKNOWLEDGMENTS

We acknowledge funding from the California Energy Commission (CEC), contract manager Prab Sethi, through the California Solar Energy Collaborative.

6. REFERENCES

1. Cano, D., J. M. Monget, M. Albuisson, H. Guillard, N. Regas and L. Wald (1986). A method for the determination of the global solar radiation from meteorological satellite data. *Solar Energy* **37** (1)

2. CIMIS (2010). California Irrigation Management Information System: CIMIS Data. Available online <http://wwwcimis.water.gov/cimis/data.jsp>. Accessed on 01/25/2010

3. Lorenz, E., J. Hurka, D. Heinemann, H. G. Beyer (2009). Irradiance forecasting for the power prediction of grid-connected photovoltaic systems. *IEEE Journal of Selected Topics in Applied Earth Observations and Remote Sensing* **2** (1)

4. Martins, F.R., E.B. Pereira and S.L. Abreu (2007). Satellite-derived solar resource maps for Brazil under SWERA project. *Solar Energy* **81**

5. NCDC (2008). Data documentation for data set 3505 (DSI-3505) integrated surface data. National Climatic Data Center, NESDIS, NOAA, U.S. Department of Commerce. Available online <http://idn.ceos.org/KeywordSearch/Metadata.do?Portal=GCMD&KeywordPath=[Sensor_Name%3A+Short_Name%3D%27AWS%27]&OrigMetadataNode=GCMD&EntryId=gov.noaa.ncdc.C00532&MetadataView=Full&MetadataType=0&lbnode=mdlb3 >. Accessed on 01/25/2010

6. Nottrott, A. and Jan Kleissl (2010). Validation of the SUNY NSRDB irradiance dataset in California. *Solar Energy* **(In Review)**

7. Perez, R., P. Ineichen, K. Moore, M. Kmiecik, C. Chain, R. George and F. Bignola (2002). A new operational satellite-to-irradiance model. *Solar Energy* **73** (5)

8. Randel, D., T. H. V. Harr, M. A. Ringerud, G. L. Stephens, T. J. Greenwald and C. L. Combs (1996). A new global water vapor dataset. *Bulletin of the American Meteorological Society* **77** (6)

9. Schmetz, J (1989). Towards a surface radiation climatology: Retrieval of downward irradiances from satellites. *Atmos. Res.* **23** (3-4)

10. Snyder, R. L. and S. Eching (2002). Penman-Monteith (hourly) reference evapotranspiration equations for estimation ETos and ETrs with hourly weather data. Available online <http://biomet.ucdavis.edu/Evapotranspiration/PMhrXLS/PMhrDoc.pdf >. Accessed on 01/25/2010

11. Sudradjat, A., R. Ferraro and M. Fiorino (2005). A comparison of total precipitable water between reanalyses and NVAP. *Journal of Climate* **18** (1)

12. Zelenka, A., R. Perez, R. Seals and D. Renné (1999). Effective accuracy of satellite-derived hourly irradiances. *Theoretical and Applied Climatology* **62**